JACS
JOURNAL OF THE AMERICAN CHEMICAL SOCIETY
pubs.acs.org/JACS
Article

Strong Surface Hydration and Salt Resistant Mechanism of a New Nonfouling Zwitterionic Polymer Based on Protein Stabilizer TMAO

Hao Huang,[#] Chengcheng Zhang,[#] Ralph Crisci, Tieyi Lu, Hsiang-Chieh Hung, Md Symon Jahan Sajib, Pranab Sarker, Jinrong Ma, Tao Wei,[*] Shaoyi Jiang,[*] and Zhan Chen[*]

Cite This: *J. Am. Chem. Soc.* 2021, 143, 16786–16795

ABSTRACT: Zwitterionic polymers exhibit excellent nonfouling performance due to their strong surface hydrations. However, salt molecules may severely reduce the surface hydrations of typical zwitterionic polymers, making the application of these polymers in real biological and marine environments challenging. Recently, a new zwitterionic polymer brush based on the protein stabilizer trimethylamine *N*-oxide (TMAO) was developed as an outstanding nonfouling material. Using surface-sensitive sum frequency generation (SFG) vibrational spectroscopy, we investigated the surface hydration of TMAO polymer brushes (pTMAO) and the effects of salts and proteins on such surface hydration. It was discovered that exposure to highly concentrated salt solutions such as seawater only moderately reduced surface hydration. This superior resistance to salt effects compared to other zwitterionic polymers is due to the shorter distance between the positively and negatively charged groups, thus a smaller dipole in pTMAO and strong hydration around TMAO zwitterion. This results in strong bonding interactions between the O^- in pTMAO and water, and weaker interaction between O^- and metal cations due to the strong repulsion from the N^+ and hydration water. Computer simulations at quantum and atomistic scales were performed to support SFG analyses. In addition to the salt effect, it was discovered that exposure to proteins in seawater exerted minimal influence on the pTMAO surface hydration, indicating complete exclusion of protein attachment. The excellent nonfouling performance of pTMAO originates from its extremely strong surface hydration that exhibits effective resistance to disruptions induced by salts and proteins.

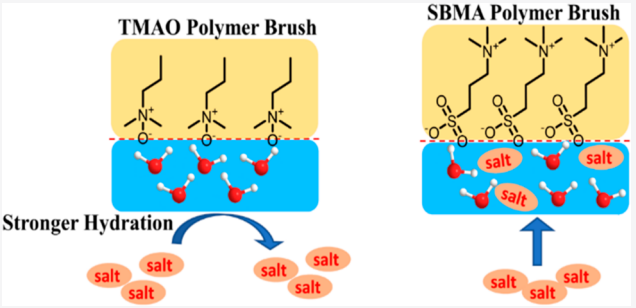

INTRODUCTION

Nonfouling polymers have been extensively developed for various applications, such as biofouling resistant coatings for many materials and devices, ranging from small medical implants to giant vessel hulls.[1−10] Among a variety of widely investigated nonfouling polymers, zwitterionic polymers were found to be promising candidates.[11−17] A zwitterionic molecule has both positively charged and negatively charged groups with the overall net charge of zero. Sulfobetaine methacrylate (SBMA) or carboxybetaine methacrylate (CBMA) has been used as a basis for developing many zwitterionic polymers in a variety of studies.[11−17] It has been thoroughly demonstrated that the strong surface hydration plays a significant role in determining the excellent nonfouling properties of zwitterionic polymers. This strong surface hydration is caused by the strong interactions between surface charges and water molecules at the zwitterionic polymer surface, leading to an ordered and strongly hydrogen bonded water layer at the polymer surface.[18−23] This water layer forms an elevated physical and energy barrier to prevent foulants from adhering to the surface. Alternatively, by simply mixing positively charged and negatively charged components in a polymer with a ratio of 1:1, a mixed charged polymer with excellent nonfouling property was recently developed with simpler synthetic procedure and lower cost.[24−26]

For nonfouling materials designed for use in biomedical applications or marine environments, it is imperative to study their performance in solutions with high salt concentrations. For example, seawater is a complex mixture, with an average salinity of ∼3.5%, which can be mimicked by a 0.6 M NaCl solution. However, when our previously studied zwitterionic and mixed charged polymers were placed in contact with concentrated salt solutions, the surface hydrations on these materials were dramatically reduced, compromising their nonfouling efficacies.[19,26] Therefore, to develop effective nonfouling coatings for practical applications, it is necessary

Received: August 16, 2021
Published: September 28, 2021

to reduce the disturbance of surface hydration caused by salt molecules.

Trimethylamine *N*-oxide (TMAO) is a zwitterionic molecule in which the positively charged N^+ and negatively charged O^- are directly bonded to each other. As a natural protein stabilizer, TMAO has been extensively researched.[27−34] It protects living cells from high urea concentration and high salinity. These unique characteristics provided us the impetus to develop advanced nonfouling materials based on TMAO. In this work, we investigated a TMAO polymer brush (pTMAO) where the TMAO molecules were covalently connected to the side chains of the polymer (Figure 1).

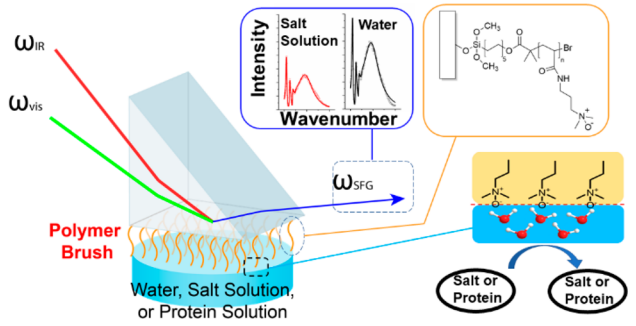

Figure 1. Left: SFG sample geometry used to study the pTMAO/water interface or the pTMAO/solution interface. Right (top left): Representative SFG spectra collected from interfaces. Top right: Molecular formula of pTMAO. The repeating unit of TMAO is represented by *n*. Bottom right: Schematic showing the interface between pTMAO and water or solutions.

To gain understanding of the surface hydration of pTMAO, a surface-sensitive technique that can directly access the interface between pTMAO and water (or solutions) is needed. Unfortunately, many surface sensitive techniques require high vacuum to operate; therefore they cannot be applied to this research because the aqueous environment cannot be achieved in high vacuum. We have applied a nonlinear optical laser technique, sum frequency generation (SFG) vibrational spectroscopy to study polymer surface structures in aqueous environment in situ as well as molecular interactions between polymers and biological molecules.[35−40] Additionally, we have also investigated interfacial water structure and found that strong surface hydration plays an important role in nonfouling.[18−23,26,41] This can be experimentally observed via a strong signal at ∼3200 cm^{-1} in the SFG spectrum collected from a nonfouling polymer/water interface. In contrast, for polymers that are not nonfouling, weakly hydrogen-bonded water may also be observed at the polymer/water interface, producing a peak at ∼3400 cm^{-1} in the SFG spectrum.[21] In this work, we used SFG to examine hydration of pTMAO in water, in salt solutions, in seawater, and in protein solutions in seawater. SFG has been applied to study TMAO hydration, and excellent results have been obtained;[27,42,43] however, this research is the first to study polymers synthesized based on TMAO. Here we first applied SFG to study surface hydration of pTMAO in water and in salt solutions with different salt concentrations (including seawater). Interestingly, pTMAO exhibits much greater resistance to concentrated salt solutions than previously studied zwitterionic polymers and mixed charged polymers. We then used computer simulations to study the TMAO−water interactions and the pTMAO/water and pTMAO/NaCl solution interfaces to further understand the surface hydration of pTMAO and related salt resistance. In addition to the pTMAO/salt solution interfaces, we also examined the interactions between pTMAO and various protein molecules in seawater using SFG. The presence of protein molecules in seawater was revealed to exert minimal influences on the surface hydration of pTMAO, demonstrating the effective nonfouling property of pTMAO in seawater. Computer simulations at quantum and atomistic scales were performed to study the hydration of the TMAO zwitterion and its interactions with the salts. Atomistic simulations on protein−pTMAO interactions were also performed to provide well correlated results to the conclusions obtained from experimental studies. Our research demonstrates that pTMAO is an excellent candidate as a nonfouling material, especially for applications in high salinity aqueous environment in biomedical and marine nonfouling applications.

METHODOLOGY

Experimental Section. The TMAO polymer brushes (pTMAO) were synthesized on right-angle silica prism (Altos Photonics, Bozeman, MT) surfaces using surface-initiated atom transfer radical polymerization (SI-ATRP).[44] In brief, a self-assembled monomer layer (SAM) was formed on each prism by soaking clean silica prisms in a (11-(2-bromo-2-methyl)propionyloxy)undecyltrichlorosilane solution (0.1% in anhydrous toluene) for 15 min. The initiator coated prisms, together with copper(I) bromide (14.35 mg, 0.1 mmol) and 1 mL of methanol, were then placed into a Schlenk tube and deoxygenated via pump-vacuum for 10 cycles. TMAO monomer (1.72 g, 10 mmol), Me6TREN (23 mg, 0.1 mmol), methanol (2.6 mL), and H_2O (0.4 mL) were added into the Schlenk tube and deoxygenated via pump-vacuum for 10 cycles. The mixed aqueous solution of TMAO monomer and Me6TREN was then transferred to the tube containing the prisms and copper bromide. The reaction was kept running at ambient temperature overnight. Afterward, the silica prisms were removed from the solution and washed with ethanol and water three times respectively and air-dried before being used for SFG study. The coated pTMAO was measured to be 20−25 nm thick using ellipsometry. Figure 1 illustrates the chemical structure of the pTMAO polymer brush. The nonfouling behavior of pTMAO in water has been confirmed using surface plasmon resonance with undiluted serum and plasma.

SFG spectroscopy was applied to probe surface hydration of pTMAO in various environments. SFG spectra were collected from the interfaces between pTMAO and various aqueous solutions including water, NaCl solutions, $MgCl_2$ solutions, seawater and protein solutions (solutions of bovine serum albumin (BSA), fibrinogen (FIB), and lysozyme (LYS)). The SFG sample geometry is shown in Figure 1. Seawater from Gulf of Mexico (S9148), BSA (99%), FIB (type I-S, 65−85%, may contain 10% sodium citrate and 15% sodium chloride), and LYS (90%) were purchased from Sigma-Aldrich. SFG theories, instrumentation, data collection, and data analysis have been extensively reported previously;[39,40,45−56] therefore they will not be repeated in detail in this article. In our SFG experiments, a green laser at 532 nm and a wavelength tunable IR laser were used as input beams and overlapped at the polymer surface or polymer/aqueous solution interface. SFG signal can only be generated from a surface or interface due to the selection rule of the SFG technique under the electric dipole approximation. The selection rule determines that only the regions where inversion symmetry is broken, i.e., at surface or interface, can contribute SFG signals. The SFG signal can be enhanced at specific input IR frequencies which are associated with vibrational transitions of the sample molecules on surface/at interface. As a result, we can characterize the molecular structure at surface or interface in situ and in real time with SFG spectroscopy.

For each SFG data set acquired, SFG signal from the polymer/water interface was collected first. We then replaced the water with

https://doi.org/10.1021/jacs.1c08280
J. Am. Chem. Soc. 2021, 143, 16786−16795

aqueous solutions (salt solutions or protein solutions) and collected SFG signals from polymer/aqueous solution interfaces. Finally, we replaced the aqueous solution with water several times and collected SFG signal from the polymer/water interface again to see if the SFG signal can recover to that of the original polymer/water interface. In this work, all SFG spectra were acquired with the ssp (s-polarized SFG signal, s-polarized green input laser beam, and p-polarized IR laser beam) polarization combination.

Computer Simulation. To further understand the strong hydration of pTMAO in water and its resistance to salt influence, computer simulations were performed. Interactions between water molecules and a single TMAO molecule in water were calculated using the ab initio molecular dynamics (AIMD) simulation with the Car−Parrinello method[57] implemented in the Quantum ESPRESSO[58] (version 6.3). A solvated TMAO molecule surrounded by 119 water molecules in a fixed cubic periodic box of the length of 16.2 Å was pursued. The AIMD calculation was accomplished by utilizing norm-conserving pseudopotentials, BYLP-parametrized generalized gradient approximation (BYLP-GGA),[59,60] and empirical Grimme DFT-D2 method[61] to incorporate van der Waals corrections, with a time step of 0.121 fs. The initial geometry of the TMAO·119H_2O system was obtained from the atomistic MD, using GROMACS (version 2019.6) with the CHARMM36 force field[62] and TIP3P water model. Partial charges of pTMAO chains were estimated using quantum simulations and the restrained electrostatic potential method as illustrated in section S1 of the Supporting Information. The careful investigation of the ionic effect on the single TMAO's hydration, with the same concentration as in the experiment, requires statistics with an extensive system and a longer time scale, which are not obtainable via a computationally expensive AIMD framework. We thus utilized atomistic MD simulation instead with the models reported in the literature[63] to study the ionic effect on a single TMAO molecule's hydration. In addition, an atomistic MD simulation was also adopted to study the pTMAO's surface hydration in water and in salt solution, as well as the protein adsorption resistance of pTMAO in salt solution. More computational details are presented in section S1 in the Supporting Information.

For simulations on pTMAO, the pTMAO brush surface used for the atomistic MD simulations was designed by connecting four TMAO with a hydroxylated α-cristobalite (101) crystal unit with an alkyl spacer, $-(CH_2)_{10}$, followed by periodical expansion. The charges for pTMAO chains were calculated using quantum calculations (see Figure S1 in the Supporting Information), while those for the hydroxylated α-cristobalite substrate were adopted from the literature.[64,65] Positions of silicon and oxygen of the substrate were fixed, whereas all others were mobile. Initially, the system was equilibrated for 13 ns by constraining the protein before the full relaxation. The final production run of 190 ns was obtained by integrating the dynamic equation with a time step of 1 fs at 300 K. More details of the atomistic MD computations are shown in section S1 in the Supporting Information.

To analyze water distribution surrounding a single TMAO molecule or near the pTMAO brush surface, we computed the normalized water concentration referring to the bulk water density using the proximal radial distribution function $pG(r)$,[66] where r is the minimum distance between a water and an atom of TMAO or pTMAO brush surface. To characterize the structure of interfacial water on pTMAO, we computed the order parameter $S = \frac{3\langle\cos^2\theta\rangle - 1}{2}$, where θ is an angle between the water dipole moment and the Z-axis which is normal to the brush surfaces, and the angle brackets represent the time average.

RESULTS AND DISCUSSION

Strong Hydration and Salt Resistant Mechanism. To investigate the surface hydration of the pTMAO, SFG spectra were first acquired from the pTMAO/water interfaces using three pTMAO samples of the same pTMAO polymer prepared in the same way (Figure 2a1, b1, c1). We noticed that this SFG spectrum is consistently dominated by the peak at about 3200 cm^{-1} contributed by the strongly hydrogen-bonded water molecules at the interface. As we reported previously, strong surface hydration is critical to the efficacy of nonfouling polymers.[18−23,41] As other zwitterionic polymers, pTMAO strongly binds with water molecules, preventing other molecules and organisms from replacing water to attach to the polymer surface. Therefore, the surface hydration of pTMAO creates a barrier to resist biofouling. In addition to the strong O−H stretching signals, strong C−H stretching signals centered at around 2895, 2950, and 2970 cm^{-1} were also detected, which are contributed by various functional groups such as $N-CH_2$, $N-CH_3$, and $C-CH_3$ groups. The C−H stretching signals in the SFG spectra collected from the pTMAO/water interfaces show some variability, which is discussed in more detail in the Supporting Information section S2. To study salt effects on the polymer surface hydration, SFG spectra were then collected from the pTMAO/concentrated salt solution interfaces. Solutions with different NaCl concentrations of 0.5 and 0.6 M, as well as seawater, were tested (Figure 2). SFG spectra of water molecules at various interfaces have been extensively investigated. For a neutral (or not charged) interface, SFG water signals are contributed by the second-order nonlinear susceptibility $\chi^{(2)}$ of the probed interfacial water molecules that adopt preferred orientations.[45−47] Therefore, the interfacial water structure can be deduced from the SFG spectra. However, for a charged interface, SFG water signals can be contributed by both the $\chi^{(2)}$ of the interfacial water (e.g., bound water molecules at an interface) as well as the third-order nonlinear susceptibility $\chi^{(3)}$ of some water molecules in the diffused layer in the water bulk near the charged interfaces. These bulk water molecules can also adopt preferred orientations due to the electric field. Such SFG signals produced by both $\chi^{(2)}$ and $\chi^{(3)}$ contributions have been well studied.[67−74]

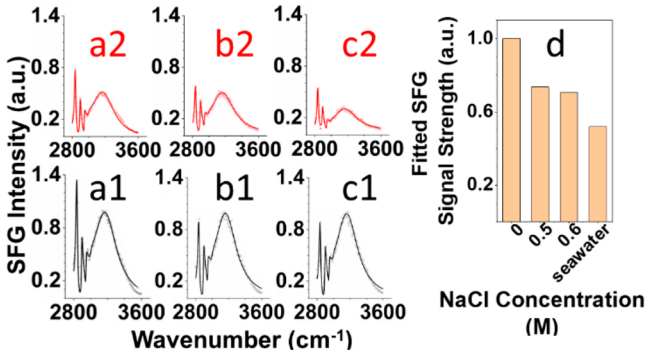

Figure 2. SFG spectra collected from the interfaces between pTMAO and water (a1, b1, c1), NaCl solutions with salt concentrations of 0.5 M (a2) and 0.6 M (b2), as well as seawater (c2). In a1, a2, b1, b2, c1, and c2, dots are experimental data and lines are fitting results. The SFG signal strengths obtained from fitting results are shown in (d).

Although ideally zwitterionic polymers such as pTMAO should be neutral, at polymer/water interfaces the positively and negatively charged functional groups can be segregated in different degrees, leading to unequal distribution of charge density. Multiple ζ-potential measurements previously conducted for sulfobetaine and carboxybetaine-based zwitterionic polymers have shown that such polymer surfaces are not completely neutral; instead, some small electric potentials can be measured on these zwitterionic polymer surfaces.[75−79] Indeed, our previous research using SFG demonstrated the

https://doi.org/10.1021/jacs.1c08280
J. Am. Chem. Soc. 2021, 143, 16786−16795

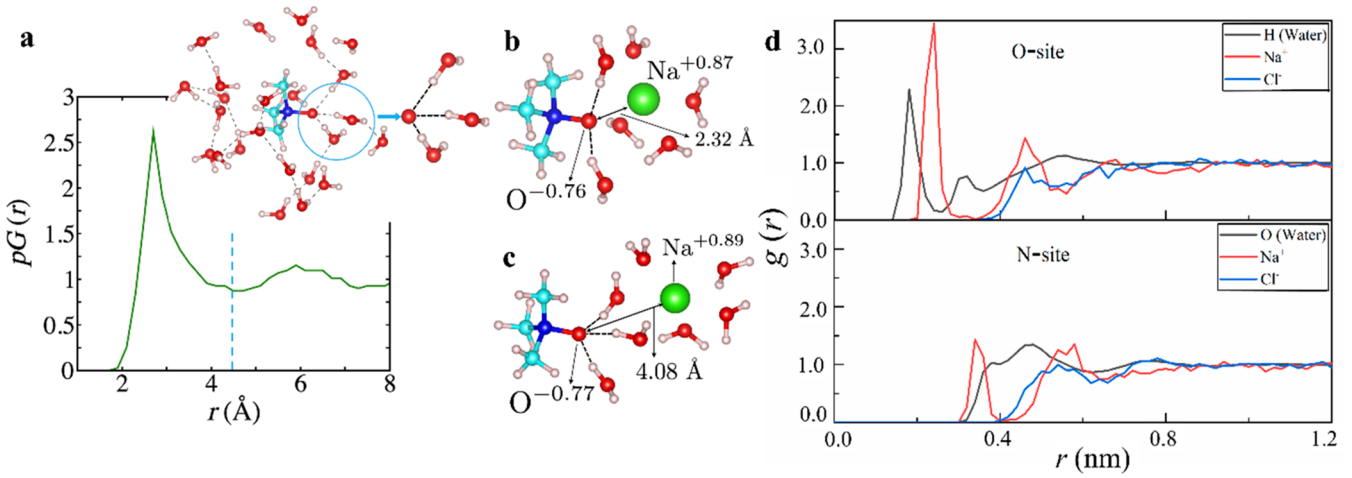

Figure 3. (a) Proximal radial distribution function ($pG(r)$) of water around a TMAO molecule and the snapshot of a TMAO surrounded by its hydration water within the first hydration shell indicated with a dash line in AIMD simulation; (b) snapshot of the direct contact of a Na^+ ion with TMAO oxygen simulated in AIMD; (c) snapshot of the indirect contact of a Na^+ ion with TMAO oxygen simulated in AIMD; (d) radial distribution $g(r)$ of hydrogen of water and ions of Na^+ and Cl^- around TMAO O-site and N-site in 0.6 M NaCl solution simulated in atomistic MD.

opposite absolute water molecule orientations on poly-SBMA (pSBMA) and poly-CBMA (pCBMA) surfaces, due to opposite overall charges on these two zwitterionic polymer surfaces.[22] Therefore, the SFG signals collected from zwitterionic polymer surfaces in water including those presented in this work can be contributed by both $\chi^{(2)}$ and $\chi^{(3)}$ effects. Since the SFG water signal contributed by the $\chi^{(2)}$ term is associated with the bonding interactions between polymer brushes and interfacial water (i.e., the surface hydration), it is necessary to deconvolute the relative contributions of $\chi^{(2)}$ and $\chi^{(3)}$ to gain accurate understandings of the surface water molecular structures on zwitterionic materials. At a charged solid/salt solution interface, if the salt concentration in the solution is minimal, SFG water signals collected from the interface are dominated by the $\chi^{(2)}$ effect.[67] Therefore, SFG spectra shown in Figure 2a1, 2b1, and 2c1 are contributed by interfacial water molecules bound to the pTMAO surface. The dominating strongly hydrogen bonded 3180 cm^{-1} peak and the absence of the ~3400 cm^{-1} weakly hydrogen bonded signal indicate strong hydration on the pTMAO surface, similar to those observed from other previously studied zwitterionic pSBMA and poly(carboxybetaine acrylamide) (pCBAA) surfaces surfaces.[18−23] It has been demonstrated in the literature that for SFG spectra collected from a charged surface/salt solution interfaces, the $\chi^{(3)}$ contribution is negligible when salt concentration in the solution is very high, due to the very strong charge screening effect.[67] Therefore, the SFG spectra collected from the pTMAO/NaCl solution interfaces (0.5 and 0.6 M) and the pTMAO/seawater interfaces (Figure 2a2, b2, and c2) are mostly contributed by the interfacial water molecules (the $\chi^{(2)}$ effect), not the $\chi^{(3)}$−effect from water molecules in the diffused layer. That is to say, relatively strong hydration was detected on the pTMAO surface even when it was brought into contact with concentrated salt solutions. It is worth noting that the SFG signal strength is proportional to the square root of the SFG signal intensity. The SFG signal strengths obtained from the fitting results of the SFG spectra collected from interfaces between pTMAO and water, NaCl solutions, and seawater are displayed in Figure 2d, indicating that the hydration strength at the pTMAO/seawater interface is not very different from that at the pTMAO/water interface (more details of the spectral fitting results are presented in the Supporting Information, section S3). This observation is very different from the previously studied zwitterionic polymer/salt solution interfaces, which will be discussed further in more detail below. In pTMAO, the distance between the negatively charged oxygen and positively charged nitrogen is very short. Due to the presence of the methyl groups surrounding N^+ on pTMAO, only O^- moiety is exposed to the solution. There is no direct interaction between N^+ and water. Because of such a short distance between O^- and N^+ groups, Na^+ and other ions do not have very strong interactions with O^- because of the repulsion with the neighboring N^+.

When the salt solution in contact with pTMAO was switched back to water, the SFG spectrum recovered (Supporting Information, section S4), indicating that the salt effect is reversible. Therefore, when the polymer contacted with salt was returned to water, the salt ions left the pTMAO surface and any possible conformation changes caused by the salt were undone, leading to the same SFG spectrum as that originally collected from the polymer/water interface. Overall these results demonstrate that the surface hydration of pTMAO could resist the disruption caused by ions in the salt solutions. Therefore, pTMAO can be used as an effective nonfouling coating material for biomedical and marine applications.

To complement the SFG experimental results and the above interpretation regarding the strong hydration of pTMAO surface in water, we first analyzed the hydration of a small TMAO zwitterionic molecule in pure water and in a 0.6 M NaCl solution, using AIMD and atomistic MD simulations (Figure 3). This single-molecule hydration serves as a model for the hydration of pTMAO surface. Both simulations consistently show that a TMAO zwitterion is surrounded by ~28 hydration water within the first hydration shell, which extends up to 4.3 Å, where the proximal radial distribution function $pG(r)$ has its first valley in pure water (Figure 3a). Among the hydration water, approximately three (coordination number = 3.0) are hydrogen-bonded (HB) with the oxygen

https://doi.org/10.1021/jacs.1c08280
J. Am. Chem. Soc. 2021, 143, 16786−16795

atom of TMAO (Figure 3a). About 25 non-HB water molecules are found to surround near the methyl groups within the first hydration shell (Figure 3a). Unlike the exposed oxygen atom, the TMAO nitrogen atom is shielded by three methyl groups and does not contact the surrounding water molecules. As such, the water molecules that directly interact with the TMAO oxygen atom play a key role in TMAO's strong hydration. Our results about TMAO hydration (HB and non-HB) are consistent with previous simulation and experimental studies.[27,80,81]

A comparison of the peak heights of ions' radial distribution $g(r)$ around O- and N-sites of TMAO shows that more Na^+ cations are associated with TMAO compared to Cl^- anions. The $g(r)$ profile of Na^+ cations has a dominant peak at a shorter distance spanning at 2.0−3.4 Å and a small peak farther away in 3.5−5.4 Å around the O-site of TMAO. The monovalent Na^+ cations are thus more likely to have direct contact with a TMAO oxygen (Figure 3b) rather than indirect contact via their hydration water (Figure 3c). The direct contact of a Na^+ cation with the O^- site of TMAO leads to the replacement of one HB water of TMAO. This replacement of HB water by Na^+ is not a frequent event as the coordination numbers of Na^+ cations show, which is 0.034 for the direct contact (the radial distance $r \leq 3.4$ Å) and 0.15 for the total of direct and indirect contacts ($r \leq 5.6$ Å) around the TMAO O-site (see Table S1 in the Supporting Information). Near the N-site, both Na^+ and Cl^- also have small coordination numbers (0.033 for Na^+ and 0.193 for Cl^-) (see Table S2 in the Supporting Information). This indicates that the TMAO hydration shell presents a barrier for Na^+ cations to access the O^- site of TMAO, and the addition of NaCl salts has a small effect on the TMAO hydration content. It is notable that the radial distribution function $g(r)$ represents the normalized local density in respect to the bulk concentration. Although $g(r)$ shows stronger peaks for ions compared to water hydrogen and oxygen (Figure 3d), due to large bulk density of water, the total amount of ions around TMAO is indeed smaller than that of water (Figure S2 in the Supporting Information). It is worth mentioning that although the hydration of TMAO has been extensively studied,[27,80−82] we believe that this is the first time the salt effect on TMAO surface hydration has been investigated. Our AIMD simulation showed the charge transfers of both Na^+ and the TMAO oxygen to the local environment are small in the case of the Na^+ direct contact (Figure 3c,d).

We also performed MD simulations on pTMAO/water and pTMAO/salt solution interfaces. The atomistic MD results presented in Figure 4a validate the strong hydration of pTMAO surfaces in both water and 0.6 M NaCl solution. A slight difference in the pTMAO surface hydration density, i.e., $pG(r)$ profile, was detected in the two cases (peak height = 2.64 for the case of pure water and peak height = 2.50 for the case of 0.6 M NaCl in Figure 4a). To quantify the ordering of the interfacial hydration water, we computed the order parameter S_{water} of water molecules at difference locations. Our analysis shows that in consistency with the SFG experimental results, interfacial water molecules in both cases exhibit ordered structures. However, the addition of NaCl (0.6 M) slightly decreased interfacial water molecules ordering (see S_{water} profile in Figure 4b) compared to the pTMAO/pure water interface. Most TMAO terminal groups were found to position on the top of the pTMAO brush surface (Figure S3 in the Supporting Information). Due to the high surface packing

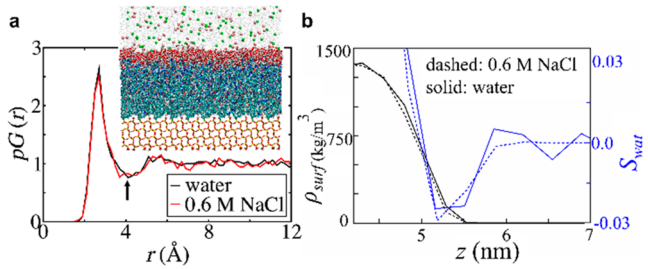

Figure 4. (a) $pG(r)$ of a pTMAO surface in the water and 0.6 M NaCl solution, drawn using the final 20 ns MD simulation data. The inset shows the equilibrated pTMAO/water interface. Red beads represent water molecules within the first hydration shell (i.e., the cutoff distance is up to the valley of $pG(r)$ indicated with a black arrow). The bulk water is colored gray. Na^+ and Cl^- ions are represented with red and green beads, respectively. The surface density is 2.4 TMAO chains/nm^2, and the repeating unit (n) is 4. (b) Densities of pTMAO (ρ_{surf}) (black) and water ordering parameter S_{water} as a function of position across the pTMAO/water interface calculated by MD simulation (solid line, the system with pure water; broken line, the system with 0.6 M NaCl).

density, the addition of NaCl salts has negligible effects on the surface thickness and surface composition (i.e., oxygen and nitrogen density profile as shown in Figure S3 in the Supporting Information). In addition, simulations show that more O^- atoms of pTMAO surface are exposed to the bulk water than N^+ atoms (see Figure S3 in the Supporting Information) due to the shielding of the nitrogen atom by methyl groups. It is worth mentioning that even for a loosely packed pTMAO brush sample, substantial water ordering in 0.6 M NaCl solution can be seen from simulation, indicating the strong surface hydration of pTMAO in salt solutions (Figure S4 in the Supporting Information).

Resistance to Protein Adsorption in Seawater. To further understand the nonfouling mechanisms of pTMAO and its resistance to the salt effect, we also studied the impact of proteins on pTMAO surface hydration using SFG. SFG experiments were conducted to study interfaces between pTMAO and solutions of three proteins: BSA, FIB, and LYS in seawater. SFG spectra were collected from the three pTMAO/protein solution interfaces, where the $\chi^{(3)}$ contributions were minimized by the high salt concentration in seawater (Figure 5). The SFG signals collected from the three pTMAO/protein

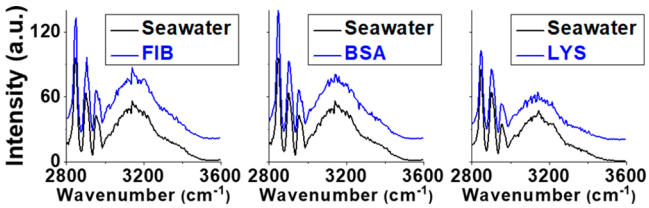

Figure 5. SFG spectra collected from the pTMAO/seawater interfaces and pTMAO/protein solution (in seawater, offset by 20 in intensity) interfaces.

solution interfaces in seawater are very similar to the ones collected from the pTMAO/seawater interface without proteins, indicating that the presence of protein molecules induces negligible influences on the surface hydration or interfacial water $\chi^{(2)}$ of pTMAO. The SFG results are also well correlated to the following recently reported research data.[44] It was shown that hydrogels made from TMAO exhibit excellent

https://doi.org/10.1021/jacs.1c08280
J. Am. Chem. Soc. 2021, 143, 16786−16795

nonfouling property against fibrinogen adhesion and complement activation and fibroblast adhesion.[44] Similarly, pTMAO polymer brush also demonstrated less than 3 ng/cm^2 protein adsorption in undiluted human blood serum.[44] Overall, these results demonstrate that pTMAO is an excellent candidate as a nonfouling material for marine and biomedical applications. Below we present a computational validation of pTMAO's nonfouling efficacy by simulating the LYS protein interacting with pTMAO in a 0.6 M NaCl solution (to model seawater).

Figure 6 shows the results of atomistic MD simulations which provide molecular insight into lysozyme's behavior at

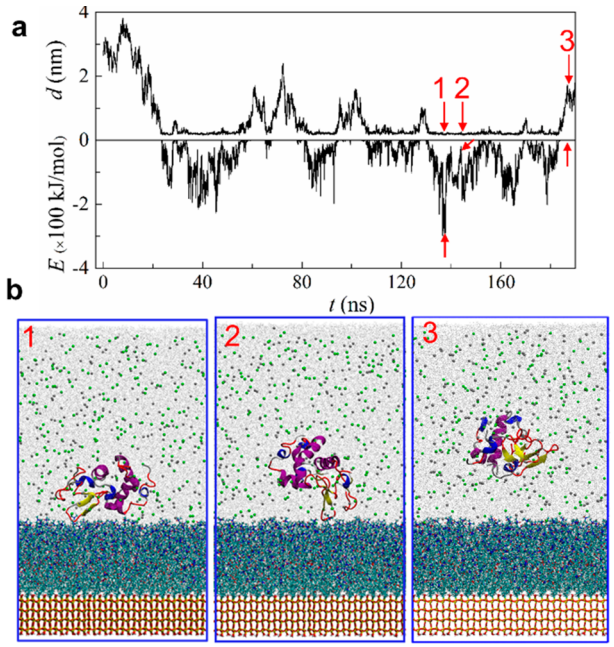

Figure 6. (a) (Up) Minimum distance (d) and (down) total interaction energy (E) between LYS protein and surface atoms as a function of time (t). (b) Protein's pTMAO surface attaching-bumping events: (1) side-on landing, (2) end-on landing, and (3) bumping away.

the pTMAO surface in a 0.6 M NaCl solution. The minimum distance between the lysozyme protein and the pTMAO surface and their interactions, including the electrostatic and van der Waals (vdW) interactions, were monitored for 190 ns (Figure 6a). Simulation results show that a lysozyme protein of a net positive charge (+8e) displays a slightly larger electrostatic interaction with the pTMAO surface than the vdW interaction (Figure S5 in the Supporting Information). During this period of 190 ns, the LYS protein came close (<0.1 nm) to and then went away from the surface multiple times, establishing the robust nonfouling nature of the pTMAO surface. The protein displayed large translational and rotational mobility on the pTMAO brush surface. For example, even when the interaction energy between pTMAO and LYS reached the highest value (~300 kJ/mol) at about 140 ns (while LYS landed on pTMAO with the long-axis parallel to the surface (side-on landing) in Figure 6b, left), LYS could not settle down on the pTMAO surface. The pTMAO's strong hydration barrier, indicated by the $pG(r)$ in Figure 3a and observed by SFG (Figure 1), enabled LYS to change the direction of its long axis, resulting in its landings with the terminal group on the surface (end-on landing) (see Figure 6b, middle). Such landings lowered the LYS−pTMAO surface interaction energies, and eventually, LYS bumped away from pTMAO (Figure 6b, right). It is notable that this mobile interfacial behavior of the protein on the nonfouling pTMAO surface is totally different from the protein adsorption behavior of LYS on our previously studied surfaces, such as azobenzene brush surfaces on the same silica substrate,[65] other surfaces of graphene,[83] gold crystal,[84,85] and polyethylene.[66,86] On these surfaces, even though the adsorption could be orientation dependent, the protein could not display large interfacial mobility due to the lack of sufficient energy barrier of surface hydration.[65,83,84] This again demonstrates the significant role that pTMAO's strong surface hydration plays in nonfouling. To validate the simulation results on lysozyme−pTMAO interactions in 0.6 M NaCl solution, we performed four additional simulation runs (each with more than 150 ns) using different initial orientations. None of these cases showed protein adsorption on pTMAO.

Further Discussion and Comparison to Other Zwitterionic Polymers. Previous SFG studies on carboxybetaine and sulfobetaine-based zwitterionic polymers as well as mixed charged polymers indicated that in DI water, strong SFG O−H stretching signals at ~3200 cm^{-1} were detected, showing strong surface hydration.[18−23] However, exposure of these materials to NaCl solutions greatly reduced the water SFG signal intensities. For example, SFG spectra collected from the interfaces between 0.5 M NaCl solution and pSBMA or 1:1 mixed charged polymer are shown in the Supporting Information, section S5 (Figure S8), which present minimum SFG O−H stretching signals.[26] In such highly concentrated salt solutions, the $\chi^{(3)}$ effect is minimized. The very weak water SFG signals are dominated by only $\chi^{(2)}$ contribution. Therefore, the surface hydrations of these previously investigated zwitterionic materials are very weak in concentrated salt solutions. This comparison demonstrates that pTMAO exhibits a uniquely strong resistance to disturbance by salts, making pTMAO a superior nonfouling coating candidate for marine and biological environments.

In addition to NaCl, we also investigated the effect of $MgCl_2$ on the surface hydration of pTMAO. Divalent metal ions are expected to have stronger binding affinity with the negatively charged groups on the polymer surface, thus reducing the hydrogen bonding of the polymer with water more substantially compared to monovalent metal ions. This was observed previously for other zwitterionic polymers such as pSBMA and pCBAAs.[19] Exposure to a very low concentration (1 mM) of $MgCl_2$ solution could greatly reduce the surface hydration of pSBMA and pCBAAs. Here even at much higher $MgCl_2$ solution concentrations (0.02 and 0.1 M), surface hydration only decreased moderately, which is seen as a moderate signal decrease in the SFG spectra (Figure S9 in the Supporting Information, section S6). This again demonstrates the very strong resistance of pTMAO surface hydration to salt disturbance.

As discussed above, in pTMAO, the distance between the negatively charged oxygen and positively charged nitrogen is very short, which is much shorter than the distances between the positively and negatively charged groups in pCBAAs (between N^+ and COO^-) and pSBMA (between N^+ and SO_3^-). Because of such short distance in pTMAO, ions do not have very strong interactions with O^- because of the repulsion with the neighboring N^+. However, due to the long distance between the negatively and positively charged sites on pCBAAs and pSBMA, Na^+ or other metal ions can more easily interact

https://doi.org/10.1021/jacs.1c08280
J. Am. Chem. Soc. 2021, 143, 16786−16795

with the negatively charged COO^- or SO_3^- sites to screen the charge effect. Previous studies have shown that the ability of the quaternary amine to order water molecules is much weaker than COO^-.[87] Therefore, the surface hydrations of pCBAAs and pSBMA can be significantly reduced by salt molecules. This explains the superior resistance of pTMAO surface hydration to disruptions caused by the salt effect.

CONCLUSIONS

In this work, we investigated TMAO polymer brush surface hydration and its resistance to the disruption caused by salt and protein. SFG spectra collected from the pTMAO/water interface revealed strongly hydrogen-bonded water layers on the pTMAO surface. NaCl solution, $MgCl_2$ solution, and seawater were used to study salt effects on pTMAO surface hydration. Surprisingly, it was found that the pTMAO surface hydration was highly resistant to the disturbance caused by salts, even in seawater. In addition to the effects of salts, the impacts of protein molecules on the pTMAO surface hydration were also tested. The three protein solutions exerted negligible impact on the surface hydration of pTMAO in seawater. MD simulations were performed to validate the SFG experimental results. The data obtained from computer simulations are well correlated to the SFG results, providing further details regarding the strong surface hydration of pTMAO in water, in salt solutions, in seawater, and in protein solution.

In comparison to previously studied zwitterionic polymers (sulfobetaine and caboxybetaine) and mixed charged polymers, the surface of pTMAO demonstrated superior resistance against hydration loss induced by salt. This is due to the short distance between the negatively charged and positively charged groups in pTMAO. This short distance leads to less charge screening effect of Na^+ and other metal ions by reducing their interactions with O^-, due to the repulsion between the neighboring N^+ in pTMAO and the cations. A lesson we can learn from this study is that when the distance between the negative and positive charges in a zwitterionic material is long, the negative and positive sites are more venerable and easier to be attacked by other ions in the solution. To resist such ion or salt effect, it is required to ensure that the distance between charges is short.

To the best of our knowledge, pTMAO is the first zwitterionic material that shows strong surface hydration in highly concentrated salt solutions. The very strong resistance of pTMAO surface hydration to salt and protein disturbances makes pTMAO a promising nonfouling material for marine environments and for biomedical applications.

ASSOCIATED CONTENT

Supporting Information

The Supporting Information is available free of charge at https://pubs.acs.org/doi/10.1021/jacs.1c08280.

Details of the computer simulations on TMAO and pTMAO, distribution of water and ions near TMAO, the coordination numbers of water hydrogen and ions around the oxygen and nitrogen of TMAO, the density distribution of nitrogen and oxygen of TMAO on the surface, surface hydration of pTMAO with low packing density, protein−surface interactions, SFG spectra of TMAO in air, water, and $MgCl_2$ solution, SFG spectra fitting results, and a comparison to other zwitterionic materials (PDF)

AUTHOR INFORMATION

Corresponding Authors

Tao Wei − *Department of Chemical Engineering, Howard University, Washington, D.C. 20059, United States;* orcid.org/0000-0001-6888-1658; Email: tao.wei@howard.edu

Shaoyi Jiang − *Meinig School of Biomedical Engineering, Cornell University, Ithaca, New York 14853, United States;* orcid.org/0000-0001-9863-6899; Email: sj19@cornell.edu

Zhan Chen − *Department of Chemistry and Applied Physics Program, University of Michigan, Ann Arbor, Michigan 48109, United States;* orcid.org/0000-0001-8687-8348; Email: zhanc@umich.edu

Authors

Hao Huang − *Department of Chemistry and Applied Physics Program, University of Michigan, Ann Arbor, Michigan 48109, United States*

Chengcheng Zhang − *Department of Chemistry, University of Michigan, Ann Arbor, Michigan 48109, United States;* orcid.org/0000-0002-3484-2519

Ralph Crisci − *Department of Chemistry, University of Michigan, Ann Arbor, Michigan 48109, United States*

Tieyi Lu − *Department of Chemistry, University of Michigan, Ann Arbor, Michigan 48109, United States*

Hsiang-Chieh Hung − *Department of Chemical Engineering, University of Washington, Seattle, Washington 98195, United States*

Md Symon Jahan Sajib − *Department of Chemical Engineering, Howard University, Washington, D.C. 20059, United States*

Pranab Sarker − *Department of Chemical Engineering, Howard University, Washington, D.C. 20059, United States*

Jinrong Ma − *Department of Chemical Engineering, University of Washington, Seattle, Washington 98195, United States*

Complete contact information is available at: https://pubs.acs.org/10.1021/jacs.1c08280

Author Contributions

#H.H. and C.Z. contributed equally.

Notes

The authors declare no competing financial interest.

ACKNOWLEDGMENTS

The authors acknowledge the support from the Office of Naval Research Award N00014-20-1-2234 (to Z.C.), Grants N00014-20-1-2731 and N00014-19-1-2063 (to S.J.), and Grant N00014-21-1-2215 (to T.W.). T.W. is grateful for the computational resources from the program of Extreme Science and Engineering Discovery Environment (XSEDE) and the Texas Advanced Computing Center (TACC).

REFERENCES

(1) Grozea, C. M.; Walker, G. C. Approaches in Designing Non-toxic Polymer Surfaces to Deter Marine Biofouling. *Soft Matter* **2009**, *5* (21), 4088−4100.

(2) Lejars, M.; Margaillan, A.; Bressy, C. Fouling Release Coatings: A Nontoxic Alternative to Biocidal Antifouling Coatings. *Chem. Rev.* **2012**, *112* (8), 4347−4390.

(3) Wei, Q.; Becherer, T.; Angioletti-Uberti, S.; Dzubiella, J.; Wischke, C.; Neffe, A. T.; Lendlein, A.; Ballauff, M.; Haag, R. Protein

Interactions with Polymer Coatings and Biomaterials. *Angew. Chem., Int. Ed.* **2014**, *53* (31), 8004−8031.
(4) Prime, K. L.; Whitesides, G. M. Adsorption of Proteins onto Surfaces Containing End-attached Oligo (ethylene oxide): A Model System Using Self-assembled Monolayers. *J. Am. Chem. Soc.* **1993**, *115* (23), 10714−10721.
(5) Gudipati, C. S.; Finlay, J. A.; Callow, J. A.; Callow, M. E.; Wooley, K. L. The Antifouling and Fouling-release Perfomance of Hyperbranched Fluoropolymer (HBFP)− Poly (ethylene glycol)-(PEG) Composite Coatings Evaluated by Adsorption of Biomacromolecules and the Green Fouling Alga Ulva. *Langmuir* **2005**, *21* (7), 3044−3053.
(6) Colak, S.; Tew, G. N. Amphiphilic Polybetaines: The Effect of Side-Chain Hydrophobicity on Protein Adsorption. *Biomacromolecules* **2012**, *13* (5), 1233−1239.
(7) Zhao, X.; Su, Y.; Li, Y.; Zhang, R.; Zhao, J.; Jiang, Z. Engineering Amphiphilic Membrane Surfaces Based on PEO and PDMS Segments for Improved Antifouling Performances. *J. Membr. Sci.* **2014**, *450*, 111−123.
(8) Liu, S. Q.; Yang, C.; Huang, Y.; Ding, X.; Li, Y.; Fan, W. M.; Hedrick, J. L.; Yang, Y. Y. Antimicrobial and Antifouling Hydrogels Formed in Situ from Polycarbonate and Poly (ethylene glycol) via Michael Addition. *Adv. Mater.* **2012**, *24* (48), 6484−6489.
(9) Brown, M. U.; Triozzi, A.; Emrick, T. Polymer Zwitterions with Phosphonium Cations. *J. Am. Chem. Soc.* **2021**, *143* (17), 6528−6532.
(10) Chen, Q.; Yu, S.; Zhang, D.; Zhang, W.; Zhang, H.; Zou, J.; Mao, Z.; Yuan, Y.; Gao, C.; Liu, R. Impact of Antifouling PEG Layer on the Performance of Functional Peptides in Regulating Cell Behaviors. *J. Am. Chem. Soc.* **2019**, *141* (42), 16772−16780.
(11) Schlenoff, J. B. Zwitteration: Coating Surfaces with Zwitterionic Functionality to Reduce Nonspecific Adsorption. *Langmuir* **2014**, *30* (32), 9625−9636.
(12) Zhang, Z.; Chao, T.; Chen, S.; Jiang, S. Superlow Fouling Sulfobetaine and Carboxybetaine Polymers on Glass Slides. *Langmuir* **2006**, *22* (24), 10072−10077.
(13) Galvin, C. J.; Dimitriou, M. D.; Satija, S. K.; Genzer, J. Swelling of Polyelectrolyte and Polyzwitterion Brushes by Humid Vapors. *J. Am. Chem. Soc.* **2014**, *136* (36), 12737−12745.
(14) Zhang, L.; Cao, Z.; Bai, T.; Carr, L.; Ella-Menye, J.-R.; Irvin, C.; Ratner, B. D.; Jiang, S. Zwitterionic Hydrogels Implanted in Mice Resist the Foreign-body Reaction. *Nat. Biotechnol.* **2013**, *31* (6), 553−556.
(15) Jiang, S.; Cao, Z. Ultralow-fouling, Functionalizable, and Hydrolyzable Zwitterionic Materials and Their Derivatives for Biological Applications. *Adv. Mater.* **2010**, *22* (9), 920−932.
(16) Ladd, J.; Zhang, Z.; Chen, S.; Hower, J. C.; Jiang, S. Zwitterionic Polymers Exhibiting High Resistance to Nonspecific Protein Adsorption from Human Serum and Plasma. *Biomacromolecules* **2008**, *9* (5), 1357−1361.
(17) Liu, Y.; Zhang, D.; Ren, B.; Gong, X.; Xu, L.; Feng, Z.-Q.; Chang, Y.; He, Y.; Zheng, J. Molecular Simulations and Understanding of Antifouling Zwitterionic Polymer Brushes. *J. Mater. Chem. B* **2020**, *8* (17), 3814−3828.
(18) Leng, C.; Sun, S.; Zhang, K.; Jiang, S.; Chen, Z. Molecular Level Studies on Interfacial Hydration of Zwitterionic and Other Antifouling Polymers in Situ. *Acta Biomater.* **2016**, *40*, 6−15.
(19) Leng, C.; Han, X.; Shao, Q.; Zhu, Y.; Li, Y.; Jiang, S.; Chen, Z. In Situ Probing of the Surface Hydration of Zwitterionic Polymer Brushes: Structural and Environmental Effects. *J. Phys. Chem. C* **2014**, *118* (29), 15840−15845.
(20) Leng, C.; Hung, H.-C.; Sun, S.; Wang, D.; Li, Y.; Jiang, S.; Chen, Z. Probing the Surface Hydration of Nonfouling Zwitterionic and PEG Materials in Contact with Proteins. *ACS Appl. Mater. Interfaces* **2015**, *7* (30), 16881−16888.
(21) Leng, C.; Hung, H.-C.; Sieggreen, O. A.; Li, Y.; Jiang, S.; Chen, Z. Probing the Surface Hydration of Nonfouling Zwitterionic and Poly(ethylene glycol) Materials with Isotopic Dilution Spectroscopy. *J. Phys. Chem. C* **2015**, *119* (16), 8775−8780.
(22) Han, X.; Leng, C.; Shao, Q.; Jiang, S.; Chen, Z. Absolute Orientations of Water Molecules at Zwitterionic Polymer Interfaces and Interfacial Dynamics after Salt Exposure. *Langmuir* **2019**, *35* (5), 1327−1334.
(23) Del Grosso, C. A.; Leng, C.; Zhang, K.; Hung, H.-C.; Jiang, S.; Chen, Z.; Wilker, J. J. Surface Hydration for Antifouling and Bioadhesion. *Chem. Sci.* **2020**, *11* (38), 10367−10377.
(24) Chen, S.; Jiang, S. An New Avenue to Nonfouling Materials. *Adv. Mater.* **2008**, *20* (2), 335−338.
(25) Mi, L.; Bernards, M. T.; Cheng, G.; Yu, Q.; Jiang, S. pH Responsive Properties of Non-fouling Mixed-charge Polymer Brushes Based on Quaternary Amine and Carboxylic Acid Monomers. *Biomaterials* **2010**, *31* (10), 2919−2925.
(26) Leng, C.; Huang, H.; Zhang, K.; Hung, H.-C.; Xu, Y.; Li, Y.; Jiang, S.; Chen, Z. Effect of Surface Hydration on Antifouling Properties of Mixed Charged Polymers. *Langmuir* **2018**, *34* (22), 6538−6545.
(27) Ohto, T.; Backus, E. H.; Mizukami, W.; Hunger, J.; Bonn, M.; Nagata, Y. Unveiling the Amphiphilic Nature of TMAO by Vibrational Sum Frequency Generation Spectroscopy. *J. Phys. Chem. C* **2016**, *120* (31), 17435−17443.
(28) Bruce, E. E.; van der Vegt, N. F. Molecular Scale Solvation in Complex Solutions. *J. Am. Chem. Soc.* **2019**, *141* (33), 12948−12956.
(29) Ganguly, P.; Boserman, P.; Van Der Vegt, N. F.; Shea, J.-E. Trimethylamine N-oxide Counteracts Urea Denaturation by Inhibiting Protein−Urea Preferential Interaction. *J. Am. Chem. Soc.* **2018**, *140* (1), 483−492.
(30) Mondal, J.; Halverson, D.; Li, I. T.; Stirnemann, G.; Walker, G. C.; Berne, B. J. How Osmolytes Influence Hydrophobic Polymer Conformations: A Unified View from Experiment and Theory. *Proc. Natl. Acad. Sci. U. S. A.* **2015**, *112* (30), 9270−9275.
(31) Ganguly, P.; Polák, J.; van der Vegt, N. F.; Heyda, J.; Shea, J.-E. Protein Stability in TMAO and Mixed Urea−TMAO Solutions. *J. Phys. Chem. B* **2020**, *124* (29), 6181−6197.
(32) Wei, H.; Fan, Y.; Gao, Y. Q. Effects of Urea, Tetramethyl Urea, and Trimethylamine N-oxide on Aqueous Solution Structure and Solvation of Protein Backbones: A Molecular Dynamics Simulation Study. *J. Phys. Chem. B* **2010**, *114* (1), 557−568.
(33) Ma, J.; Pazos, I. M.; Gai, F. Microscopic Insights into the Protein-Stabilizing Effect of Trimethylamine N-oxide (TMAO). *Proc. Natl. Acad. Sci. U. S. A.* **2014**, *111* (23), 8476−8481.
(34) Smolin, N.; Voloshin, V. P.; Anikeenko, A. V.; Geiger, A.; Winter, R.; Medvedev, N. N. TMAO and Urea in the Hydration Shell of the Protein SNase. *Phys. Chem. Chem. Phys.* **2017**, *19* (9), 6345−6357.
(35) Chen, C.; Wang, J.; Loch, C. L.; Ahn, D.; Chen, Z. Demonstrating the Feasibility of Monitoring the Molecular-level Structures of Moving Polymer/Silane Interfaces during Silane Diffusion Using SFG. *J. Am. Chem. Soc.* **2004**, *126* (4), 1174−1179.
(36) Lu, X.; Zhang, C.; Ulrich, N.; Xiao, M.; Ma, Y.-H.; Chen, Z. Studying Polymer Surfaces and Interfaces with Sum Frequency Generation Vibrational Spectroscopy. *Anal. Chem.* **2017**, *89* (1), 466−489.
(37) Lu, X.; Clarke, M. L.; Li, D.; Wang, X.; Xue, G.; Chen, Z. A Sum Frequency Generation Vibrational Study of the Interference Effect in Poly (n-butyl methacrylate) Thin Films Sandwiched between Silica and Water. *J. Phys. Chem. C* **2011**, *115* (28), 13759−13767.
(38) Chen, X.; Wang, J.; Paszti, Z.; Wang, F.; Schrauben, J. N.; Tarabara, V. V.; Schmaier, A. H.; Chen, Z. Ordered Adsorption of Coagulation Factor XII on Negatively Charged Polymer Surfaces Probed by Sum Frequency Generation Vibrational Spectroscopy. *Anal. Bioanal. Chem.* **2007**, *388* (1), 65−72.
(39) Wang, J.; Woodcock, S. E.; Buck, S. M.; Chen, C.; Chen, Z. Different Surface-restructuring Behaviors of Poly (methacrylate)s Detected by SFG in Water. *J. Am. Chem. Soc.* **2001**, *123* (38), 9470−9471.
(40) Wang, J.; Paszti, Z.; Even, M. A.; Chen, Z. Measuring Polymer Surface Ordering Differences in Air and Water by Sum Frequency

https://doi.org/10.1021/jacs.1c08280
J. Am. Chem. Soc. 2021, 143, 16786−16795

Generation Vibrational Spectroscopy. *J. Am. Chem. Soc.* **2002**, *124* (24), 7016−7023.
(41) Leng, C.; Gibney, K. A.; Liu, Y.; Tew, G. N.; Chen, Z. In Situ Probing the Surface Restructuring of Antibiofouling Amphiphilic Polybetaines in Water. *ACS Macro Lett.* **2013**, *2* (11), 1011−1015.
(42) Sagle, L. B.; Cimatu, K.; Litosh, V. A.; Liu, Y.; Flores, S. C.; Chen, X.; Yu, B.; Cremer, P. S. Methyl Groups of Trimethylamine N-oxide Orient Away from Hydrophobic Interfaces. *J. Am. Chem. Soc.* **2011**, *133* (46), 18707−18712.
(43) Ahmed, M.; Namboodiri, V.; Mathi, P.; Singh, A. K.; Mondal, J. A. How Osmolyte and Denaturant Affect Water at the Air−Water Interface and in Bulk: A Heterodyne-detected Vibrational Sum Frequency Generation (HD-VSFG) and Hydration Shell Spectroscopic Study. *J. Phys. Chem. C* **2016**, *120* (19), 10252−10260.
(44) Li, B.; Jain, P.; Ma, J.; Smith, J. K.; Yuan, Z.; Hung, H.-C.; He, Y.; Lin, X.; Wu, K.; Pfaendtner, J.; Jiang, S. Trimethylamine N-oxide-derived Zwitterionic Polymers: A New Class of Ultralow Fouling Bioinspired Materials. *Sci. Adv.* **2019**, *5* (6), eaaw9562.
(45) Lambert, A. G.; Davies, P. B.; Neivandt, D. J. Implementing the Theory of Sum Frequency Generation Vibrational Spectroscopy: A Tutorial Review. *Appl. Spectrosc. Rev.* **2005**, *40* (2), 103−145.
(46) Shen, Y. R. Basic Theory of Surface Sum-Frequency Generation. *J. Phys. Chem. C* **2012**, *116* (29), 15505−15509.
(47) Perry, A.; Neipert, C.; Space, B.; Moore, P. B. Theoretical Modeling of Interface Specific Vibrational Spectroscopy: Methods and Applications to Aqueous Interfaces. *Chem. Rev.* **2006**, *106* (4), 1234−1258.
(48) Wang, J.; Buck, S. M.; Even, M. A.; Chen, Z. Molecular Responses of Proteins at Different Interfacial Environments Detected by Sum Frequency Generation Vibrational Spectroscopy. *J. Am. Chem. Soc.* **2002**, *124* (44), 13302−13305.
(49) Tuladhar, A.; Dewan, S.; Pezzotti, S.; Brigiano, F. S.; Creazzo, F.; Gaigeot, M.-P.; Borguet, E. Ions Tune Interfacial Water Structure and Modulate Hydrophobic Interactions at Silica Surfaces. *J. Am. Chem. Soc.* **2020**, *142* (15), 6991−7000.
(50) Hu, D.; Chou, K. C. Re-evaluating the Surface Tension Analysis of Polyelectrolyte-Surfactant Mixtures Using Phase-Sensitive Sum Frequency Generation Spectroscopy. *J. Am. Chem. Soc.* **2014**, *136* (43), 15114−15117.
(51) Xiao, M.; Wei, S.; Chen, J.; Tian, J.; Brooks, C. L., Iii; Marsh, E. N. G.; Chen, Z. Molecular Mechanisms of Interactions between Monolayered Transition Metal Dichalcogenides and Biological Molecules. *J. Am. Chem. Soc.* **2019**, *141* (25), 9980−9988.
(52) Wei, S.; Zou, X.; Tian, J.; Huang, H.; Guo, W.; Chen, Z. Control of Protein Conformation and Orientation on Graphene. *J. Am. Chem. Soc.* **2019**, *141* (51), 20335−20343.
(53) Kataoka, S.; Cremer, P. S. Probing Molecular Structure at Interfaces for Comparison with Bulk Solution Behavior: Water/2-propanol Mixtures Monitored by Vibrational Sum Frequency Spectroscopy. *J. Am. Chem. Soc.* **2006**, *128* (16), 5516−5522.
(54) Tan, J.; Zhang, J.; Luo, Y.; Ye, S. Misfolding of a Human Islet Amyloid Polypeptide at the Lipid Membrane Populates through β-sheet Conformers without Involving α-helical Intermediates. *J. Am. Chem. Soc.* **2019**, *141* (5), 1941−1948.
(55) Chen, X.; Sagle, L. B.; Cremer, P. S. Urea Orientation at Protein Surfaces. *J. Am. Chem. Soc.* **2007**, *129* (49), 15104−15105.
(56) Ding, B.; Panahi, A.; Ho, J.-J.; Laaser, J. E.; Brooks, C. L., III; Zanni, M. T.; Chen, Z. Probing Site-specific Structural Information of Peptides at Model Membrane Interface in Situ. *J. Am. Chem. Soc.* **2015**, *137* (32), 10190−10198.
(57) Car, R.; Parrinello, M. Unified Approach for Molecular Dynamics and Density-Functional Theory. *Phys. Rev. Lett.* **1985**, *55* (22), 2471.
(58) Giannozzi, P.; Baroni, S.; Bonini, N.; Calandra, M.; Car, R.; Cavazzoni, C.; Ceresoli, D.; Chiarotti, G. L.; Cococcioni, M.; Dabo, I.; et al. Quantum ESPRESSO: A Modular and Open-source Software Project for Quantum Simulations of Materials. *J. Phys.: Condens. Matter* **2009**, *21* (39), 395502.
(59) Becke, A. D. Density-functional Exchange-energy Approximation with Correct Asymptotic Behavior. *Phys. Rev. A* **1988**, *38* (6), 3098.
(60) Miehlich, B.; Savin, A.; Stoll, H.; Preuss, H. Results Obtained with the Correlation Energy Density Functionals of Becke and Lee, Yang and Parr. *Chem. Phys. Lett.* **1989**, *157* (3), 200−206.
(61) Grimme, S. Semiempirical GGA-type Density Functional Constructed with A Long-range Dispersion Correction. *J. Comput. Chem.* **2006**, *27* (15), 1787−1799.
(62) Huang, J.; Rauscher, S.; Nawrocki, G.; Ran, T.; Feig, M.; De Groot, B. L.; Grubmüller, H.; MacKerell, A. D. CHARMM36m: An Improved Force Field for Folded and Intrinsically Disordered Proteins. *Nat. Methods* **2017**, *14* (1), 71−73.
(63) Hölzl, C.; Kibies, P.; Imoto, S.; Frach, R.; Suladze, S.; Winter, R.; Marx, D.; Horinek, D.; Kast, S. M. Design Principles for High-Pressure Force Fields: Aqueous TMAO Solutions from Ambient to Kilobar Pressures. *J. Chem. Phys.* **2016**, *144* (14), 144104.
(64) Patwardhan, S. V.; Emami, F. S.; Berry, R. J.; Jones, S. E.; Naik, R. R.; Deschaume, O.; Heinz, H.; Perry, C. C. Chemistry of Aqueous Silica Nanoparticle Surfaces and the Mechanism of Selective Peptide Adsorption. *J. Am. Chem. Soc.* **2012**, *134* (14), 6244−6256.
(65) Wei, T.; Sajib, M. S. J.; Samieegohar, M.; Ma, H.; Shing, K. Self-Assembled Monolayers of an Azobenzene Derivative on Silica and Their Interactions with Lysozyme. *Langmuir* **2015**, *31* (50), 13543−13552.
(66) Wei, T.; Carignano, M. A.; Szleifer, I. Lysozyme Adsorption on Polyethylene Surfaces: Why Are Long Simulations Needed? *Langmuir* **2011**, *27* (19), 12074−12081.
(67) Schaefer, J.; Gonella, G.; Bonn, M.; Backus, E. H. Surface-Specific Vibrational Spectroscopy of the Water/Silica Interface: Screening and Interference. *Phys. Chem. Chem. Phys.* **2017**, *19* (25), 16875−16880.
(68) Pullanchery, S.; Yang, T.; Cremer, P. S. Introduction of Positive Charges into Zwitterionic Phospholipid Monolayers Disrupts Water Structure Whereas Negative Charges Enhances It. *J. Phys. Chem. B* **2018**, *122* (51), 12260−12270.
(69) Mafi, A.; Hu, D.; Chou, K. C. Interactions of Sulfobetaine Zwitterionic Surfactants with Water on Water Surface. *Langmuir* **2016**, *32* (42), 10905−10911.
(70) Wen, Y.-C.; Zha, S.; Liu, X.; Yang, S.; Guo, P.; Shi, G.; Fang, H.; Shen, Y. R.; Tian, C. Unveiling Microscopic Structures of Charged Water Interfaces by Surface-Specific Vibrational Spectroscopy. *Phys. Rev. Lett.* **2016**, *116* (1), 016101.
(71) Dreier, L. B.; Bernhard, C.; Gonella, G.; Backus, E. H.; Bonn, M. Surface Potential of a Planar Charged Lipid−Water Interface. What Do Vibrating Plate Methods, Second Harmonic and Sum Frequency Measure? *J. Phys. Chem. Lett.* **2018**, *9* (19), 5685−5691.
(72) Urashima, S.-h.; Myalitsin, A.; Nihonyanagi, S.; Tahara, T. The Topmost Water Structure at A Charged Silica/Aqueous Interface Revealed by Heterodyne-detected Vibrational Sum Frequency Generation Spectroscopy. *J. Phys. Chem. Lett.* **2018**, *9* (14), 4109−4114.
(73) Dreier, L. B.; Nagata, Y.; Lutz, H.; Gonella, G.; Hunger, J.; Backus, E. H.; Bonn, M. Saturation of Charge-induced Water Alignment at Model Membrane Surfaces. *Sci. Adv.* **2018**, *4* (3), eaap7415.
(74) Rehl, B.; Rashwan, M.; DeWalt-Kerian, E. L.; Jarisz, T. A.; Darlington, A. M.; Hore, D. K.; Gibbs, J. M. New Insights into χ (3) Measurements: Comparing Nonresonant Second Harmonic Generation and Resonant Sum Frequency Generation at the Silica/Aqueous Electrolyte Interface. *J. Phys. Chem. C* **2019**, *123* (17), 10991−11000.
(75) Du, M.; Ma, Y.; Su, H.; Wang, X.; Zheng, Q. Rheological Behavior of Hydrophobically Modified Polysulfobetaine Methacrylate Aqueous Solution. *RSC Adv.* **2015**, *5* (43), 33905−33913.
(76) Liu, P.; Emmons, E.; Song, J. A Comparative Study of Zwitterionic Ligands-mediated Mineralization and the Potential of Mineralized Zwitterionic Matrices for Bone Tissue Engineering. *J. Mater. Chem. B* **2014**, *2* (43), 7524−7533.

https://doi.org/10.1021/jacs.1c08280
J. Am. Chem. Soc. 2021, 143, 16786−16795

(77) Mary, P.; Bendejacq, D. D.; Labeau, M.-P.; Dupuis, P. Reconciling Low-and High-salt Solution Behavior of Sulfobetaine Polyzwitterions. *J. Phys. Chem. B* **2007**, *111* (27), 7767−7777.
(78) Wu, L.; Jasinski, J.; Krishnan, S. Carboxybetaine, Sulfobetaine, and Cationic Block Copolymer Coatings: A Comparison of the Surface Properties and Antibiofouling Behavior. *J. Appl. Polym. Sci.* **2012**, *124* (3), 2154−2170.
(79) Guo, S.; Jańczewski, D.; Zhu, X.; Quintana, R.; He, T.; Neoh, K. G. Surface Charge Control for Zwitterionic Polymer Brushes: Tailoring Surface Properties to Antifouling Applications. *J. Colloid Interface Sci.* **2015**, *452*, 43−53.
(80) Sahle, C. J.; Schroer, M. A.; Niskanen, J.; Elbers, M.; Jeffries, C. M.; Sternemann, C. Hydration in Aqueous Osmolyte Solutions: the Case of TMAO and Urea. *Phys. Chem. Chem. Phys.* **2020**, *22* (20), 11614−11624.
(81) Usui, K.; Hunger, J.; Sulpizi, M.; Ohto, T.; Bonn, M.; Nagata, Y. Ab initio Liquid Water Dynamics in Aqueous TMAO Solution. *J. Phys. Chem. B* **2015**, *119* (33), 10597−10606.
(82) Zou, Q.; Bennion, B. J.; Daggett, V.; Murphy, K. P. The Molecular Mechanism of Stabilization of Proteins by TMAO and Its Ability to Counteract the Effects of Urea. *J. Am. Chem. Soc.* **2002**, *124* (7), 1192−1202.
(83) Nakano, C. M.; Ma, H.; Wei, T. Study of Lysozyme Mobility and Binding Free Energy During Adsorption on a Graphene Surface. *Appl. Phys. Lett.* **2015**, *106* (15), 153701.
(84) Wei, T.; Ma, H.; Nakano, A. Decaheme Cytochrome MtrF Adsorption and Electron Transfer on Gold Surface. *J. Phys. Chem. Lett.* **2016**, *7* (5), 929−936.
(85) Jahan Sajib, M. S.; Sarker, P.; Wei, Y.; Tao, X.; Wei, T. Protein Corona on Gold Nanoparticles Studied with Coarse-grained Simulations. *Langmuir* **2020**, *36* (44), 13356−13363.
(86) Wei, T.; Carignano, M. A.; Szleifer, I. Molecular Dynamics Simulation of Lysozyme Adsorption/Desorption on Hydrophobic Surfaces. *J. Phys. Chem. B* **2012**, *116* (34), 10189−10194.
(87) Shao, Q.; He, Y.; White, A. D.; Jiang, S. Difference in Hydration between Carboxybetaine and Sulfobetaine. *J. Phys. Chem. B* **2010**, *114* (49), 16625−16631.

https://doi.org/10.1021/jacs.1c08280
J. Am. Chem. Soc. 2021, 143, 16786−16795